Formation of multiwall fullerenes from nanodiamonds studied by atomistic simulations

Jan H. Los,[1] Nicolas Pineau,[2] Guillaume Chevrot,[2] Gérard Vignoles,[3] and Jean-Marc Leyssale[3]

[1]*LRC "Méso" CMLA, ENS Cachan, 61 Avenue du Président Wilson, 94235 Cachan Cedex, France*

[2]*CEA, DAM, DIF, F-91297 Arpajon, France*

[3]*LCTS, UMR 5801, CNRS-CEA-Snecma Propulsion Solide, Université Bordeaux 1, 3 Allée de La Boétie, 33600 Pessac, France*

The high-temperature annealing of nanodiamonds with sizes typical of ultradisperse diamonds is studied with atomistic simulations using a recent and accurate classical reactive potential. At 3000 K, the complete transformation of the particles into carbon onions made of five to seven concentric fullerenes occurs according to a three-step mechanism: (i) formation of two to three graphitic shells at the surface, (ii) transformation of the diamond core into an amorphous sp^2 carbon, and (iii) reorganization of the core into concentric fullerene layers. At lower temperatures, the transformation stops at step (i) and the final structure is made of a diamond core surrounded by a few fullerene shells. The analysis of the internal pressure of the diamond core reveals that this state is metastable.

Nanometer-sized diamonds have been observed in many carbon-rich environments, both terrestrial[1] and extraterrestrial,[2] since their discovery in meteorites.[3] Similarly to diamond, these particles experience graphitization when exposed to high temperatures[4] which results, due to the particular size and shape of nanodiamonds (NDs), in the formation of quasispherical multiwall fullerenes called carbon onions (COs).[5] Nanodiamonds obtained as detonation residues[1] are particularly interesting in that context. Indeed, because of the preparation conditions, these ultradisperse diamonds (UDDs) show very homogeneous sizes peaked around 5 nm (Ref. 6) making their fullerenization a unique process for the purpose of producing monodisperse nanoonions. UDDs are not only important from a technological point of view due to their particularly interesting tribologic and optical properties, but they also offer the opportunity to gain new insight on the diamond-graphite transition at the nanoscale where both size and shape play an important role. The thermodynamics of this process is of great interest for specific detonation applications where phase transitions can affect the equation of state of the detonation products of carbon rich explosives.[7,8] Molecular simulations and in particular *ab initio* or tight-binding-based molecular-dynamics (MD) simulations have given useful insights in the diamond-graphite transition[9] and some studies of nanodiamond annealing have been undertaken.[10,11] However, because of the high computational cost associated with *ab initio* methods, they have been limited so far to nanodiamonds of at most 1.4 nm in diameter (less than 300 atoms) which is clearly insufficient to fully capture the mechanism of onion formation from UDD precursors. Interesting simulation work, using the environment-dependent interatomic potential (EDIP) for carbon of Marks,[12] on the formation of COs from an amorphous precursor involving thousands of atoms has been recently presented in Ref. 13. This work also briefly shows the CO formation from a nanodiamond precursor, but at a high temperature of 4000 K and without giving any details of the transformation mechanism and structural details.

In a previous attempt to simulate the graphitization of nanodiamonds of realistic sizes, two of us recently performed molecular-dynamics simulations of 3–7 nm nanodiamonds at temperatures ranging from 1300 to 3000 K (Refs. 14 and 15) using the REBO2 (Ref. 16) and AIREBO (Ref. 17) empirical potentials. Results obtained with these two potentials were unsatisfactory and contradictory. The REBO2 potential gives extremely quick graphitizations, ranging from some picoseconds to a few nanoseconds depending on system size and annealing temperature. However the resulting particles have a quite dense "puffy" octahedron structure [keeping the memory of the initial (111) diamond planes], rather than spherical, onionlike structure. On the other hand, using the AIREBO potential, the annealing of a 3 nm nanodiamond for 2 ns at 3000 K leads to only very partial graphitization. These results can be rationalized by looking at the energy path of the well-known (111) diamond to rhombohedral graphite transformation[18] shown in Fig. 1 at the DFT level of theory and for different empirical models.[12,16,17,19]

We can see in Fig. 1 that the REBO2 model overestimates the barrier height, which should delay the graphitization process, but considerably underestimates its width thus facilitating the formation of onionlike structures (two graphitic
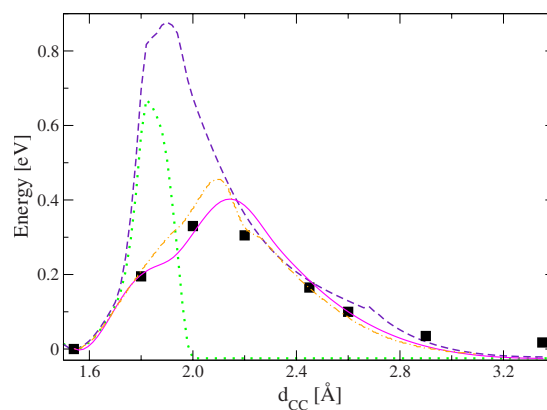

FIG. 1. (Color online) Minimum energy path for the diamond conversion to rhombohedral graphite (d_{cc} is the length of the dissociating C-C bond). Symbols: DFT results of Fahy *et al.* (Ref. 18); dotted line: REBO2 potential (Ref. 16); dashed line: AIREBO potential (Ref. 17); dashed-dotted line: EDIP potential (Ref. 12) (data taken from Ref. 20); full line: LCBOPII potential (Ref. 19).

planes can be as close as 2 Å at no energetic cost). On the opposite, despite a well-behaved tail, the AIREBO potential shows a 3 times higher barrier than DFT, making the process much too costly.

Of the potentials in Fig. 1, only the EDIP and the long-range carbon bond order potential LCBOPII properly describe the DFT barrier. These two potentials reproduce very well the shape of this energy barrier and only slightly overestimate its height, LCBOPII performing a little better on that particular point. Another advantage of LCBOPII with respect to EDIP is that it incorporates the weak interlayer van der Waals (vdW) interactions responsible, e.g., for the interlayer binding in graphite, but we admit that this may be not so crucial for studying graphitization processes from a diamond precursor.

The initial idea of LCBOP was to extend the Brenner potential with long-range (nonbonded, vdW) interactions.[21] After that, the LCBOP was further developed to make it more suitable for the liquid phase and to improve its description of all common carbon phases (graphite, diamond, fullerenes, nanotubes, graphene) and of phase transformations. In the latest version, LCBOPII, so-called middle range (MR) interactions were added to improve the reactive properties.[19] These MR interactions were fitted to *ab initio* calculations of dissociation energy curves. Different versions of the LCBOP have been successfully applied to a variety of carbon phases including the liquid phase.[22–26] The ability of this potential to accurately describe the thermodynamic phase diagram of bulk carbon as well as the barrier height of the diamond-graphite transformation makes it a perfect candidate for the simulation of nanodiamond annealing.[27,28]

We now present the results of a molecular-dynamics simulation of a 3 nm ND (2512 atoms) annealed in vacuum at a constant temperature of 3000 K during 2 ns. We used the code STAMP developed at CEA and implementing the LCBOPII potential. The temperature was controlled with a Langevin thermostat using a friction parameter of 10^{14} s^{-1} and the equations of motion were integrated with a time step of 0.5 fs. No periodic boundaries were employed so that the system consists of an isolated carbon cluster submitted to no external pressure. While the thermographitization of nanodiamonds is usually thought to proceed through a standard layer by layer mechanism,[4,29] from the surface toward the core of the particle, our simulation unravels a rather more complicated scenario. The graphitization mechanism is illustrated in Fig. 2 and can be decomposed in three distinct stages: during the first 100 ps, graphitization starts at the surface of the cluster and two outer fullerene layers are formed [Figs. 2(b) and 2(c)], then, up to 200 ps, the nanodiamond core undergoes a complete and irreversible transition from a fourfold to a highly disordered structure of threefold atoms [Fig. 2(d)]. Finally, the threefold core is transformed into three inner fullerene layers during the remaining 1.6 ns [Figs. 2(e) and 2(f)]. We monitored the time evolution of the graphitization process through the potential energy and the coordination distribution of the system (Fig. 3). The coordination of a single atom is defined as the number of nearest neighbors within a cutoff radius of 2 Å (close to the first minimum of the radial distribution function for both diamond and graphite). At the end of the simulation
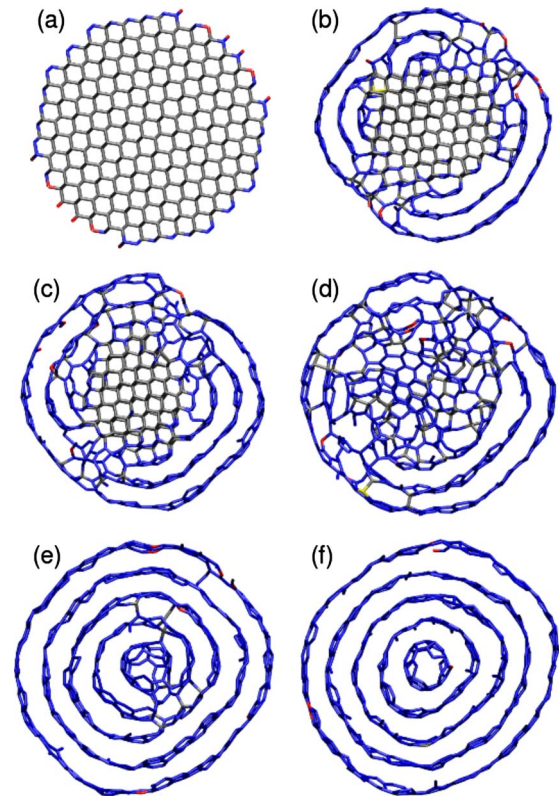

FIG. 2. (Color online) 6 Å-thick slices as a function of time (a: 0 ps, b: 50 ps, c: 100 ps, d: 200 ps, e: 800 ps, and f: 1600 ps) illustrating the graphitization mechanism of a 3 nm UDD at 3000 K. Atoms are colored according to their coordination (red: twofold, blue: threefold, gray: fourfold, yellow: other).

($\sim$2 ns), all the monitored quantities have reached a plateau implying that the system is close to equilibrium. The diamond-to-onion transition is clearly evidenced by the simultaneous decrease/increase of the fourfold/threefold coor-
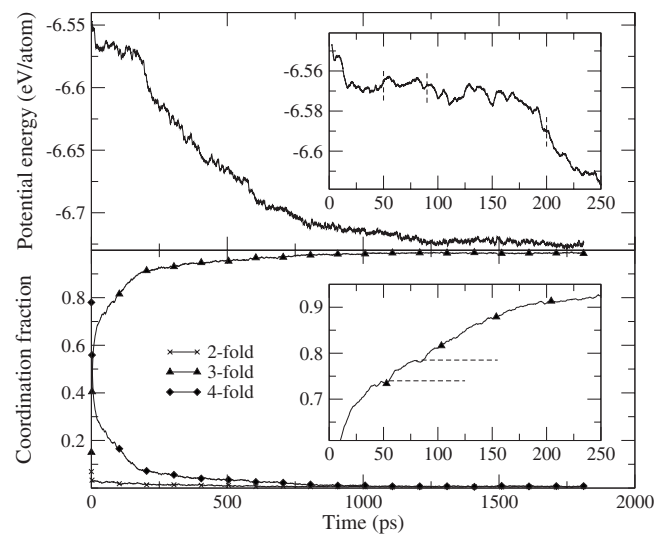

FIG. 3. Time evolution of the potential energy and coordination distribution during graphitization. Insets focus on the first 250 ps of simulation (only the threefold fraction is pictured): horizontal dotted lines highlight the presence of two plateau for the threefold fraction at $t=50$ ps and $t=90$ ps.

(a)

(b) **(c)**
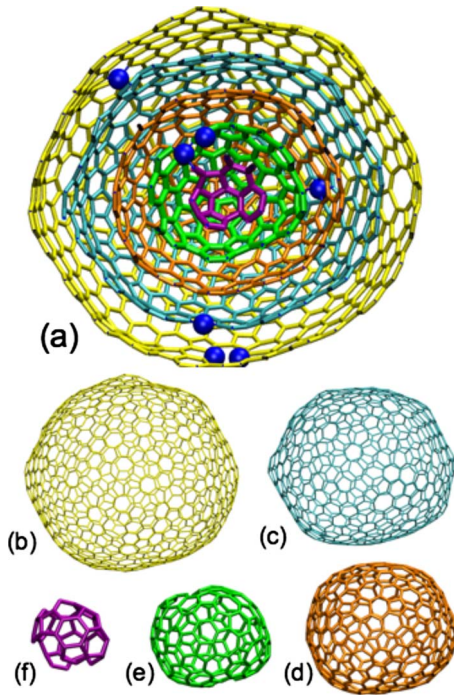
(f) **(e)** **(d)**

FIG. 4. (Color online) Carbon onion structure as identified by a cluster analysis of five to seven shortest path rings. (a) Cross section of the onion, (b) external C_{1134}, (c) C_{739}, (d) C_{405}, (e) C_{179}, and (f) internal C_{42} [only threefold atoms are considered in the analysis, the remaining sp^3 atoms are shown with large sphere in Fig. 4(a)].

dination fractions, leading to a final value of 0.98 for the threefold fractions and negligible values (inferior to 1%) for all other coordinations. The analysis of the time evolution of the threefold fraction highlights the main stages of the graphitization mechanism, with a stepwise pattern during the formation of the two outer fullerene layers (see explanation in caption of Fig. 3), and a smooth evolution during the core transition (from 0.8 to 0.9 between 100 and 200 ps). Then the threefold fraction slowly equilibrates to its final value of 0.98. Although the potential energy does not exhibit this stepwise pattern, its evolution undergoes a dramatic change when the core fullerene layers start to form. Actually, the rather weak energy decrease (≈ 20 meV/atom) during the fourfold to threefold transition suggests that entropy is the driving force for this process, while the formation of the core layers is driven by a strong energy stabilization (≈ 150 meV/atom).

Cooling the system down to 300 K, a shortest path ring (SPR) analysis[30] restricted to threefold atoms shows that the particle is typical of fullerenes and giant fullerenes with 68.8% six-member rings (C_6), 18.3% five-member rings (C_5), and 11.0% seven-member rings (C_7) [other rings found in the particle include 1.4% eight-member rings (C_8) and 0.2% four- and nine-member rings (C_4 and C_9)]. The clustering of C_5-C_7 rings into fragments of neighboring rings (those sharing at least one carbon atom) unravels the onion structure. As can be seen in Fig. 4, five quasispherical fullerenes, comprised of 1134, 739, 405, 179, and 42 three-fold atoms, are clearly identified. As for conventional fullerenes, the fraction of C_5 (respectively, C_6) rings de-
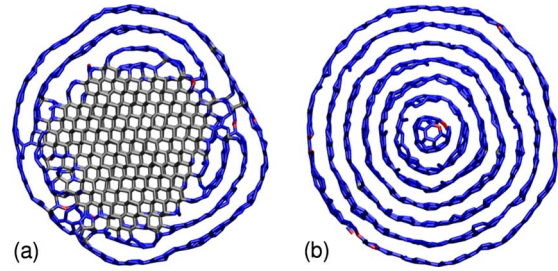

(a) **(b)**

FIG. 5. (Color online) 6 Å-thick slices of the final structures at (a) 2500 K and (b) 3000 K from (NVT) MC simulations starting from a roughly spherical nanodiamond containing $N=5851$ atoms with diameter 4.5 nm. Same color code as in Fig. 2

creases (respectively, increases) when the fullerene size increases. Indeed, the inner fullerene has the same number of C_5 and C_6 rings (i.e., five) while the outer one counts 91 C_5 and 412 C_6 rings. The fraction of seven-member rings, however, does not show any significant dependence on the fullerene size, except for the smaller one which does not count any C_7. This can be explained by the fact that the curvature in fullerenes is mainly driven by C_5 rings.

In order to assess the graphitization properties of larger clusters and to learn more about the transition temperature within shorter computation times, we also performed Metropolis Monte Carlo (MC) simulations at various temperatures with a 3 nm ND containing 2425 atoms (ND2425) and a 4 nm ND with 5851 atoms (ND5851). The temperature T was increased in steps from $T=1500$ K to $T=3000$ K via $T=2000$, 2500, and 2750 K. The initial graphitization of the surface layer proceeds rather quickly and sets in already at $T=1500$ K, but the progression of the graphitization toward the center is quite slow. For ND5851, even after 2×10^6 MC cycles at 2500 K, the aggregate still contains a large diamond core, as shown in Fig. 5(a), and the graphitization seems to have stopped, pointing toward an equilibrium coexistence of the two phases. Raising the temperature to 2750 K leads to an additional graphitic shell, but a smaller diamond core survives. Finally, after another 1.5×10^6 MC cycles at $T=3000$ K, the diamond core breaks down into an amorphous sp^2 phase, just as in the MD simulation above, and then the system completely evolves into the seven-layered onion structure shown in Fig. 5. Similar results are observed for ND2425 with a full "multiwall fullerenization" obtained only at $T=3000$ K. We add that the final structures as well as the repartition of five to seven member rings as a function of the fullerene size show very similar trends and values as those obtained through MD annealing at the same temperature.

Diamond becomes more stable than graphite at higher pressures. Therefore, the existence of a higher pressure inside the diamond core at 2500 K, partially due to the outer onion shells which constrain the available volume, might explain the resistance of the core against further graphitization. To investigate this, we have determined the pressure inside the diamond core, P_{dc}, using
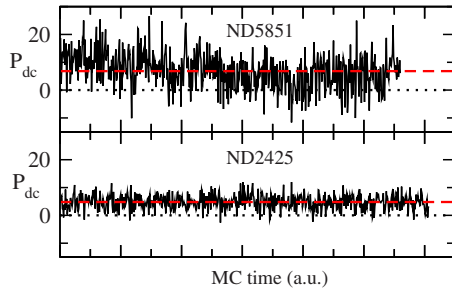
FIG. 6. (Color online) Fluctuations in the diamond core pressure P_{dc} (in GPa) as determined during MC simulations at 2500 K for the two nanoaggregates ND2425 and ND5851. Dashed line gives the average value.

$$P_{dc} = P_{dc,id} + P_{vir} = \rho_{dc} k_B T - \frac{\partial E_{dc}}{\partial V_{dc}}, \tag{1}$$

where $P_{dc,id} = \rho_{dc} k_B T$ is the ideal vapor or kinetic contribution and P_{vir} is the virial contribution. E_{dc} is the potential energy of the diamond core and ρ_{dc} its average number density. In practice, the diamond core was defined as the largest network of fourfold atoms with only fourfold neighbors. Then, E_{dc} and V_{dc} are simply evaluated as $E_{dc} = \Sigma_i^{N_{dc}} E_i$ and $V_{dc} = N_{dc}/\rho_{dc}$, with N_{dc} the number of atoms in the diamond core. Diamond having an extremely low compressibility, we used a constant ρ_{dc} value obtained from the partial radial distribution function of the diamond core.

The fluctuations of the internal pressure as determined from Eq. (1) are shown in Fig. 6 for the two nanoaggregates. The average pressures for ND2425 and ND5851 are, respectively, 6.83 ± 2.45 and 4.79 ± 0.31 GPa with much larger fluctuations observed for ND2425 due to the smaller size of its core. For the same reason, the average core pressure in ND2425 is larger than that in ND5851, in agreement with Laplace's equation which relates the pressure inside a cluster to its surface energy divided by its radius. According to the recently calculated phase diagram for LCBOPII, the equilibrium pressure for bulk diamond-graphite coexistence at 2500 K is ~12.5 GPa. For clusters, the equilibrium pressure would be even higher due to the much higher surface energy contribution for diamond. This suggests that the observed coexistence of the diamond core and the outer fullerene shells is not an equilibrium coexistence but a metastable state separated from the complete CO structure by a barrier which is considerably higher than the one shown in Fig. 1. In fact, the observed three-step transformation has little to do with this "ideal" (111)-plane diamond-graphite transformation.

After complete fullerenization at 3000 K, the average in-tershell distance is ~3.06 Å for both clusters. To compare, in graphite, a pressure of ~9.6 GPa is required to obtain a similar interlayer distance. However, using now Eq. (1) for the whole COs and with the appropriate final atomic density leads to an almost zero pressure for both particles. Using Laplace's equation, i.e., $P_{CO} = 2\gamma_{CO}/R_{CO}$, suggests that γ_{CO} is very small. Indeed, there are no broken covalent bonds at the CO surface whereas the curvature is accommodated by the presence of C_5 rings, thus without creating surface tension. In more technical detail, we find that the pressure contributions from the kinetic term and the intershell repulsion are (almost) counterbalanced by a slight dilation of the intraplanar, covalent bonds.

Summarizing, we have simulated the complete multiwall fullerenization of 3–4 nm nanodiamonds using the LCBOPII potential, both by MD and by MC simulations showing similar results. These simulations give access to unprecedented microscopic details on this interesting transformation process. First, the outer fullerene shells are formed leaving a diamond core. Then, at a sufficiently high temperature (3000 K, with respect to our accessible simulation time), the diamond core first transforms to an amorphous phase, after which the whole cluster gradually transforms itself into an almost perfect CO. Along the transformation, the considerable pressure inside the diamond core (5–7 Gpa) is released, the pressure in the final CO being negligible. This observed mechanism, involving the melting of the diamond core into an amorphous sp^2 carbon core, is different from the layer by layer graphitization usually assumed at lower temperatures.[4,29] Although more work has to be done on the kinetic aspects of the transformation, the graphitization of a 3 nm UDD at 3000 K observed in about 2 ns in this work can be related to the plasma spray experiments of Gubarevich *et al.*[31] These authors observed the full transformation of 10 nm nanodiamonds in less than 300 μs (the maximum interaction time with the plasma) with a process temperature estimated to be in the range 2700–4500 K. A more accurate comparison of the time scales is hindered by the difference in the ND sizes, the uncertainty in the experimental transformation time and temperature, as well as a possible surface passivation in the real NDs due to the presence of oxygen and hydrogen containing chemical groups. Another possible cause of discrepancy between simulated and experimentally observed transformation kinetics could be the shape of the initial diamond particle. Indeed, depending on the shape of the particle, different diamond crystal planes can be found at the particle surface which can either delay or speed-up the graphitization process. Although we used spherical particles in this work, for simplicity, other shapes such as the truncated octahedron will have to be investigated in future works.

[1] N. R. Greiner, D. S. Philips, J. D. Johnson, and F. Volk, Nature (London) **333**, 440 (1988).

[2] H. G. Hill, A. P. Jones, and L. B. d'Hendecourt, Astron. Astrophys. **336**, L41 (1998).

[3] R. S. Lewis, M. Tang, J. F. Wacker, E. Anders, and E. Steel, Nature (London) **326**, 160 (1987).

[4] V. L. Kuznetsov, A. L. Chuvilin, Y. V. Butenko, I. Y. Mal'kov, and V. M. Titov, Chem. Phys. Lett. **222**, 343 (1994).

[5] D. Ugarte, Nature (London) **359**, 707 (1992).

[6] J.-Y. Raty and G. Galli, Nature Mater. **2**, 792 (2003).

[7] J. A. Viecelli, S. Bastea, J. N. Glosli, and F. H. Ree, J. Chem. Phys. **115**, 2730 (2001).

[8] G. Chevrot, E. Bourasseau, N. Pineau, and J.-B. Maillet, Carbon **47**, 3392 (2009).

[9] A. De Vita, G. Galli, A. Canning, and R. Car, Nature (London) **379**, 523 (1996).

[10] F. Fugaciu, H. Hermann, and G. Seifert, Phys. Rev. B **60**, 10711 (1999).

[11] G.-D. Lee, C. Z. Wang, J. Yu, E. Yoon, and K. M. Ho, Phys. Rev. Lett. **91**, 265701 (2003).

[12] N. A. Marks, Phys. Rev. B **63**, 035401 (2000).

[13] D. W. M. Lau, D. G. McCulloch, N. A. Marks, N. R. Madsen, and A. V. Rode, Phys. Rev. B **75**, 233408 (2007).

[14] J.-M. Leyssale and G. L. Vignoles, Chem. Phys. Lett. **454**, 299 (2008).

[15] J.-M. Leyssale and G. L. Vignoles (unpublished).

[16] D. W. Brenner, O. A. Shenderova, J. A. Harrison, S. J. Stuart, B. Ni, and S. B. Sinnott, J. Phys.: Condens. Matter **14**, 783 (2002).

[17] S. J. Stuart, A. B. Tutein, and J. A. Harrison, J. Chem. Phys. **112**, 6472 (2000).

[18] S. Fahy, S. G. Louie, and M. L. Cohen, Phys. Rev. B **34**, 1191 (1986).

[19] J. H. Los, L. M. Ghiringhelli, E. J. Meijer, and A. Fasolino, Phys. Rev. B **72**, 214102 (2005).

[20] N. A. Marks, J. Phys.: Condens. Matter **14**, 2901 (2002).

[21] J. H. Los and A. Fasolino, Phys. Rev. B **68**, 024107 (2003).

[22] L. M. Ghiringhelli, J. H. Los, A. Fasolino, and E. J. Meijer, Phys. Rev. B **72**, 214103 (2005).

[23] L. M. Ghiringhelli, J. H. Los, E. J. Meijer, A. Fasolino, and D. Frenkel, Phys. Rev. Lett. **94**, 145701 (2005).

[24] A. Fasolino, J. H. Los, and M. I. Katsnelson, Nature Mater. **6**, 858 (2007).

[25] N. Pineau, L. Soulard, J. H. Los, and A. Fasolino, J. Chem. Phys. **129**, 024708 (2008).

[26] J. H. Los, M. I. Katsnelson, O. V. Yazyev, K. V. Zakharchenko, and A. Fasolino, Phys. Rev. B **80**, 121405(R) (2009).

[27] F. Colonna, J. H. Los, A. Fasolino, and E. J. Meijer, Phys. Rev. B **80**, 134103 (2009).

[28] N. Pineau, J. H. Los, and A. Fasolino (unpublished).

[29] Z. Qiao, J. Li, N. Zhao, C. Shi, and P. Nash, Scr. Mater. **54**, 225 (2006).

[30] D. S. Franzblau, Phys. Rev. B **44**, 4925 (1991).

[31] A. V. Gubarevich, J. Kitamura, S. Usuba, H. Yokoi, Y. Kakudate, and O. Odawara, Carbon **41**, 2601 (2003).